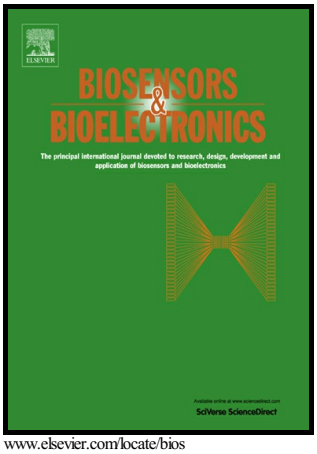


www.elsevier.com/locate/bios

# Near-Infrared Photoluminescence Biosensing Platform with Gold Nanorods-over-Gallium Arsenide Nanohorn Array

Yiming Zhang, Tao Jiang, Longhua Tang

PII: S0956-5663(17)30384-6
DOI: http://dx.doi.org/10.1016/j.bios.2017.06.009
Reference: BIOS9779

To appear in: *Biosensors and Bioelectronic*

Received date: 7 March 2017
Revised date: 24 May 2017
Accepted date: 6 June 2017

Cite this article as: Yiming Zhang, Tao Jiang and Longhua Tang, Near-Infrared Photoluminescence Biosensing Platform with Gold Nanorods-over-Gallium Arsenide Nanohorn Array, *Biosensors and Bioelectronic* http://dx.doi.org/10.1016/j.bios.2017.06.009

# Near-Infrared Photoluminescence Biosensing Platform with Gold Nanorods-over-Gallium Arsenide Nanohorn Array

Yiming Zhang[1], Tao Jiang[2], Longhua Tang[2*]

[1]School of Agricultural and Food Science, Zhejiang Agriculture and Forestry University, Lin'an, Hangzhou 311300, China

[2]State Key Laboratory of Modern Optical Instrumentation, College of Optical Science and Engineering, Zhejiang University, Hangzhou 310027, China

[*]Corresponding author: Tel: +86-571-87953066; Fax: +86-571-87956063. lhtang@zju.edu.cn



**ABSTRACT**

The near-infrared (NIR) optical detection of biomolecules with high sensitivity and reliability have been expected, however, it is still a challenge. In this work, we present a gold nanorods (AuNRs)-over-gallium arsenide nanohorn-like array (GaAs NHA) system that can be used for the ultrasensitve and specific NIR photoluminescence (PL) detection of DNA and proteins. The fabrication of GaAs NHA involved the technique of colloidal lithography and inductively

coupled plasma dry etching, yielding large-area and well-defined nanostrucural array, and exhibiting an improved PL emission compared to the planar GaAs substrate. Importantly, we found that the DNA-bridged AuNRs attachment on NHA could further improve the PL intensity from GaAs, and thereby provide the basis for the NIR optical sensing of biological analytes. We demonstrated that DNA and thrombin could be sensitively and specifically detected, with the detection limit of 1 pM for target DNA and 10 pM for thrombin. Such ultrasensitive NIR optical platform can extend to the detection of other biomarkers and is promising for clinical diagnostics.

Graphical abstract

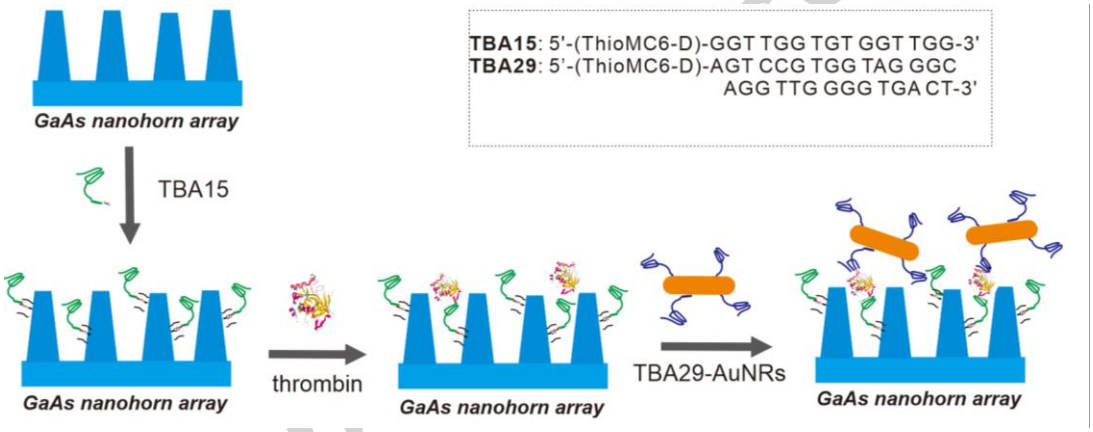


**Keywords:** gallium arsenide (GaAs); near-infrared photoluminescence; gold nanorods; biosensor; nanohorn array; DNA; thrombin

## 1. Introduction

Ultrasensitive, specific and reliable detection of biomarkers is of great importance in gene profiling, drug screening, and clinic diagnostics, because of their close association with various biological processes and diseases. In this regard, many molecular detection approaches have been developed, such as electrochemistry, colorimetry, fluorescence, surface plasmon resonance (SPR) and electric signals, etc. (Homola 2008; Liu et al. 2009; Gopinath et al. 2014; Howes et al. 2014; Song et al. 2014; Lim & Gao 2016; Smith et al. 2017). Among them, fluorescence (including photoluminescence, PL)-based assays are among the most preferred techniques in the development of biosensing systems, owing to their simple and great convenience and reliability (Homola 2008; Hilderbrand & Weissleder 2010; Howes, Rana et al. 2014). Extensive studies have focused on the integration with signal amplification strategies, and the improving on the sensing capability in the complex fluids (*e.g.*, the rapid detection of biomarkers in blood at pM concentrations), but there are still several important roadblocks that limit their practical applications. First, many analytes in real-life samples are in the complicated biological fluids (*e.g.*, blood, serum), while the fluorescence detection in complex fluid relies on extensive sampling pretreatment (*e.g.*, concentration and separation) because of the nonspecific binding, which significantly reduce the testing efficiency and accuracy (Song, Huang et al. 2014). Second, the most current state-of-the-art amplification strategies, including various isothermal amplification techniques, can offer high sensitivity and in some cases high selectivity, but often are costly, laborious and time-consuming (Connolly & Trau 2010; Guo et al. 2015). Additionally, most of the biosensors for the fluorescence detection of biomarkers were fabricated by using sandwich-type methods, in which the process are complicated and the insufficient limit of detection (LOD) significantly limit the practical applications (Gopinath, Tang et al. 2014). It

is thus very interesting and valuable to seek for a simple and robust biosensing platform for ultrasensitive detection of biomarkers.

Currently, considerable interest has focus on the near-infrared (NIR) fluorescent biosensing platforms for biological imaging and detection, as the NIR spectral range within 700–1700 nm is referred to as the "biological window", in which the light absorbance, scattering and auto-fluorescence of tissues, blood and water are at a minimum (Hilderbrand & Weissleder 2010; Malic et al. 2011; Hong et al. 2017). Thus, the biosensors operating in the NIR region can avoid interference from biological media and thereby facilitate relatively interference-free sensing. However, only a limited number of organic fluorophores, such as IRDye78, Cy7 and indocyanine green, are suitable in this range, and they also have some drawbacks such as relatively low quantum yield, easy photobleaching and broad emission spectra, which significantly limit their effectiveness in bioassays (Resch-Genger et al. 2008; Hong, Antaris et al. 2017). Semiconductor nanostructures (including quantum dots, quantum nanowires and quantum nanowells) are promising fluorescent materials for biosensors, because of their many advantages over conventional organic fluorophores such as high PL efficiency, tunable emission wavelengths narrower emission bandwidths and photostability (Gao et al. 2004; Rosini & Magri 2010; Boghossian et al. 2011). However, so far the applications of NIR semiconductor nanomaterials in biosensing and clinic diagnostics field still encounter a number of scientific and engineering challenges, such as in the controllable and reproducible detection of biomarkers with low abundance.

Owing to their excellent NIR PL and controllable surface modification, we earlier utilized gallium arsenide (GaAs) as biosensing platform to monitor the DNA hybridization events, and integrated with the DNA-decorated gold nanoparticles (AuNPs) to modulate the PL emission of

GaAs, achieving the detection of nM concentration of target DNA (Tang et al. 2013). More recently, we further depicted that the use of DNA scaffold as a bridge to control the distance of AuNPs away from GaAs, enabling a DNA length-dependent PL enhancement from GaAs (Yu et al. 2016). Actually, the integration of surface plasmons (SPs) from plasmonic nanoparticles with semiconductor nanometrials is of interest for both fundamentals study and potential applications in optics, devices and catalytic reactions. In our case, it is expected that the AuNPs would increase the density of states and the spontaneous emission in the GaAs because of the metal-enhanced fluorescence effect (Okamoto et al. 2004; Jin & Gao 2009; Zhou et al. 2009). Despite these progresses, the planar GaAs substrates have not fulfilled their promise as NIR optical sensing platform as their limited PL emission efficiency and thereby insufficient sensitivity for the detection of trace biomarkers (Tang, Chun et al. 2013). As reported, the nanostructured semiconductors normally have a higher quantum efficiency, and thus are potentially serve as a more sensitive biosensing platforms. For example, the GaAs nanowires had been synthesized and the investigation on their emission properties suggested that the higher quantum efficiency could enhance the PL emission of the semiconductor (Fortuna et al. 2008; Rosini & Magri 2010). Furthermore, compared to the flat surfaces or micron-scale pores/channels, semiconducting nanostructures with a higher porosity with submicron or nano-sized features were more favorable to loading more active biomolecules. Therefore, a three-dimensional (3D) nanostructured GaAs surface would be ideally suited for this biosensing system (Barnes, Dereux et al. 2003). To the best of our knowledge, however, little effort has been expended on the demonstration of enhanced PL emission with plasmonic NPs on the above GaAs substrates, and the further NIR optical biosensing application remains to be further explored (Barnes et al. 2003; Okamoto, Niki et al. 2004; Shahbazyan 2012; Guo, Jackman et al. 2015).

In this work, we report a gold nanorods (AuNRs)-over-GaAs nanohorn-like arrays (NHA) system for specific and ultrasensitive detection of targets of DNA and proteins. A large-area well-defined GaAs NHA nanostructure has been designed and fabricated using the colloidal NPs array-templated dry etching technique, as schematically represented in Figure 1A. We also demonstrated the nanostructured GaAs array possessed an enhanced the PL emission compared to the planar GaAs substrate, and importantly the attachment of AuNRs could further improve the PL intensity. In addition, this well-ordered and uniform nanostructured GaAs platform could provide reproducible PL signals and had high bio-recognition activity for target biomarkers. Based on these findings, we proposed the AuNRs-over-GaAs NHA systems (i.e., DNA-bridged AuNRs attachment on GaAs NHA) for enhancing the NIR PL emission, and explored their biosensing performance for biological analytes (*e.g.*, DNA and thrombin) even in the serum samples.



## 2. EXPERIMENTAL METHODS

### *2.1 Materials.*

The single-crystal $n^+$-GaAs (100) substrates used in the study were purchased from AXT, Inc. Tetrachloroauric (III) acid trihydrate ($HAuCl_4 \cdot 3H_2O$, 99.999%), L-ascorbic acid (99%), tris(2-carboxyethyl)phosphine hydrochloride (TCEP) and mercaptohexanol (MCH) were purchased from Sigma-Aldrich (China). Monodisperse silica nanospheres (NSs) with diameters of ~ 500 nm were obtained from Base Line Co. (2.5 % w/v, coefficient of variation less than 5 %). Thrombin (from human plasma), bovine serum albumin (BSA), immunoglobulin G (IgG), hemoglobin and serum were obtained from Beijing DingGuo Biotech. Co., Ltd. All other chemicals were of analytical grade and purchased from Beijing Chemical Co. (Beijing, China).

The above reagents were used without further purification and Milli-Q water (18 $M\Omega \cdot cm^{-1}$) was used to prepare all aqueous solutions. The used oligonucleotides in this study were obtained from Shanghai Sangon Biotech. Co. Ltd. and used as received.

### *2.2 Fabrication of GaAs nanohorn-like array.*

The well-defined GaAs nanohorn-like array was fabricated using colloidal lithography and inductively coupled plasma (ICP) dry etching, as schematically depicted in Figure 1a. First, a large-area uniformly-distributed colloidal array on GaAs substrate was fabricated by ethanol-assisted self-assembly (Dai et al. 2012; Liu et al. 2014). Prior to the assembly, silica NSs were separated by centrifugation, washed by excessive $H_2O$ several times and were re-dispersed in mixture of $H_2O$ and ethanol (2:1, v/v) with ultrasonication for at least 3 min. Then, the cleaned GaAs substrate was treated with oxygen plasma in ICP to improve its hydrophobicity. Afterwards, deionized water was dropped onto the wafer to form a 2 mm-thick water film. Next, the silica NSs suspension was continuously, slowly injected into the edge of the water film on GaAs substrate by a syringe pump (KD Scientific KDS200). With the assistance of ethanol, silica NSs were quickly spread on the water film and self-assembled into a monolayer at the water-air interface. After the self-assembly process, etching of GaAs was performed by ICP (Oxford Plasmalab System 100) by sequentially using reacting gases of $CF_4/CHF_3$ and $Ar/BCl_3$. The former gas of $CF_4/CHF_3$ could selectively etched the silica to increase the gaps between adjacent NSs, and the latter $Ar/BCl_3$ chemistry could selectively etch GaAs to form the eventual nanohorn-like structure.

### *2.3 Immobilization of DNA on GaAs NHA substrates.*

DNA-modified GaAs NHA substrates were fabricated as described previously (Tang, Chun et al. 2013). GaAs substrates were first cleaved into small pieces (1 cm × 1 cm) and then sequentially cleaned by $H_2O$, ethyl alcohol, acetone, and then $H_2O$. Next, the GaAs pieces were immersed in a solution of HCl–$H_2O$ (v/v, 1:10) for 1 min, then rinsed with $H_2O$. Afterwards, each GaAs was exposed to a 2 μM thiolated DNA probes or aptamers solution in PBS buffer (0.1 mM, pH 6.8) for 12 h, and then washed by $H_2O$ four times. To improve the binding efficiency of DNA onto GaAs surface, the DNA were first treated by TCEP before use. To reduce the nonspecific binding, the DNA attached GaAs was immersed in an aqueous solution of MCH (0.1 mM) for 1 h. After washing with $H_2O$, the DNA-functionalized GaAs substrates were obtained and stored in PBS solution until use.

### *2.4. Investigation of NIR PL of AuNRs-over-GaAs NHA system.*

We utilized the DNA duplex as a bridge to attach the AuNRs onto the GaAs NHA substrate according to our previous report (Yu, Li et al. 2016). As illustrated in the Scheme S1 in supplementary materials, GaAs NHA was first modified with thiolated anchoring DNA (aDNA), and then hybridized with the recognition DNA (rDNA). Next, the as-resulted DNA-modified GaAs NHA substrates were immersed into the AuNRs solution with Tris-HCl buffer (50 mM, pH 7.4) containing NaCl (100 mM) for 2 h at room temperature. After thoroughly rinsing in 50 mM NaCl, the samples were measured by PL spectroscopy. All sensing measurements were performed under excitation laser of 632 nm, acquisition time of 5 s, and 20 × objective lens.

### *2.5 Investigation of hybridization activity of DNA immobilized on GaAs NHA substrates and their sensing ability of target DNA.*

As shown in Figure 3a, probe DNA (pDNA, 5'-SH-C6-AGT CAF TGT GGA-3')-modified GaAs NHA substrates hybridized with target DNA (tDNA, 5'-GC TAG AGA TTT TCC ACA CTG ACT-3') with varying concentration and enhancer DNA (eDNA, 5'-AAA TCT CTA GC-C6-SH-3')-modified AuNRs (eDNA-AuNRs, 10 μM) in hybridization buffer (1 × PBS, 0.1% tween 20, pH 7.4). The hybridization was conducted at 37 $^{o}$C for 2 h. After hybridization, the wafers were washed with washing buffer (0.5 × PBS, 0.01% tween 20), then $H_2O$, and blown dry with $N_2$. Finally, the PL spectra of GaAs were collected. All sensing measurements were performed under excitation laser of 632 nm, acquisition time of 10 s, and 20 × objective lens.

### *2.5 NIR PL detection of thrombin using AuNRs-over-GaAs NHA platform.*

The experimental procedure typically involved the immobilization of thrombin-binding aptamers onto GaAs NHA and AuNRs respectively, interacting with thrombin and PL measurement (Figure 4a). First, two different thrombin-binding aptamers (TBA15 and TBA29) were modified onto GaAs NHA and AuNRs, respectively, resulted in the conjugations of TBA15-GaAs and TBA29-AuNRs. Then, a solution of target thrombin with varied concentration and TBA29-AuNRs was dropped onto the GaAs NHA surface to initiate the aptamer-thrombin binding events, with incubation at 37 °C for 2 h. The reaction buffer contained 10 mM PBS buffer (pH 7.0) with 100 mM NaCl, and 4 mM $Mg^{2+}$. After five washing steps to remove non-specifically bound AuNRs and other species, the samples were left to air dry and finally measured by PL microscope.

### *2.6 Characterization.*

PL spectra of GaAs were collected using a Renishaw microPL/Raman microscope, with the laser-pumping wavelength at 632 nm. For PL characterization, the excitation laser used was ~ 40

μm in spot size; when a PL intensity comparison of different samples was made, efforts were taken to ensure that multiple spots on the GaAs surface were measured. The error bars correspond to the standard deviation of PL measurements across at least ten repetitive experiments. The excitation power density was in a range of 0.05 to 4.5 kW/cm$^2$.). Scanning electron microscopy (SEM) images were obtained using a Hitachi S4800 scanning electron microscope. High-resolution transmission electron microscopy (HRTEM, Hitachi HT7700, operated at 200 kV) were used to characterize the morphology AuNRs. The absorption of AuNRs was measured on the UV-vis spectrometry (Shimadzu Co, UV-Vis 1750). Error bars represent the standard deviations for measurements taken from three-five independent experiments.

## 3. RESULTS AND DISCUSSION

### *3.1 Fabrication and characterization of GaAs nanohorn array*

The GaAs nanohorn-like array was fabricated by the combination of colloidal lithography and inductively coupled plasma (ICP) dry etching, as described in the experimental section. Typically, the silica NSs assembly on GaAs wafer had iridescent color under different angles of view (Figure 1B). The specific light diffraction indicates the formation of a periodic array on the GaAs substrate. Figure 1C presents the typical corresponding scanning electron microscopy (SEM) image. A large-area uniform monolayer of silica NSs array was clearly observed, which was in a hexagonal close-packed arrangement on the GaAs wafer. Although there are some defect or cracks in the monolayer on GaAs, by cutting the GaAs wafer into smaller pieces (*e.g.*, 10 mm × 10 mm), long defect-free and centimeter-scale sensing platform could be obtained. This high quality of the surface of the monolayer with the close-packed large spheres will assure the

next dry etching steps. After the sequential ICP etching, a uniform and well-ordered nanohorn array was formed, as observed in the side-view SEM imaging of the cross-section of GaAs substrate (Figure 1D and 1E). The resultant nanohorn structures were well-shaped with smooth side walls. Atomic force microscope (AFM) imaging was further confirmed the formation of nanohorns-like array on GaAs (Figure 1F and 1G). In addition, we have also checked the structural uniformity of the colloidal crystals in the whole sample, showing good uniformity, as typically shown in Figure S1 in supplementary materials. Due to the self-assembly technique at the water-air interface and controllable etching by ICP, the proposed approach is simple and facile to fabricate large-area and well-ordered GaAs nanohorns-like structure.

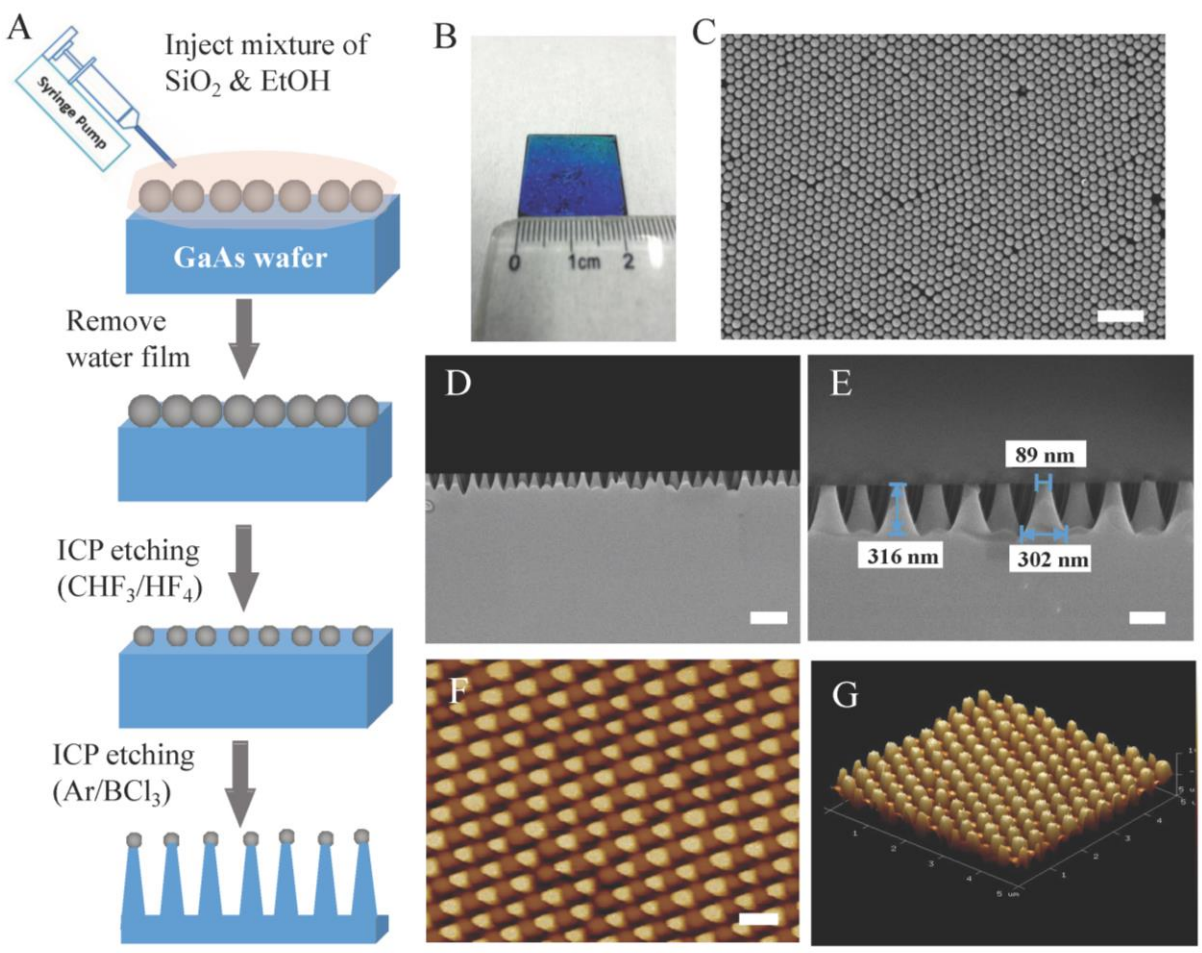

**Figure 1.** Fabrication and structure characterization of GaAs nanohorn array. (A) Schematic illustration of the fabrication approach. (B) Typical photograph and (C) SEM image of silica naonospheres monolayer on GaAs wafer. Iridescent color from the order silica naonospheres nanostructure can be clearly seen. (D, E) Cross-sectional SEM images and (F, G) AFM images of nanohorn array on GaAs. Scale bar: (C) 4 μm; (D, E, F) 200 nm.

### *3.2. Enhanced NIR PL emission of GaAs NHA with AuNRs attachment.*

Because of the 3D nanostructure of the GaAs NHA, we supposed that they have higher efficiency in the PL emission compared to the planar surface (Chun et al. 2010; Rosini & Magri 2010). To evaluate the effect of DNA modified onto the GaAs, the PL emission of GaAs NHA and thiolated DNA-modified NHA substrate were characterized (Figure 2 spectra c and e). Noted the PL peak of the pristine GaAs wafer at ~ 875 nm is normalized to 1, 5.6-fold and 8.9-fold enhancements in peak PL intensity were observed for the GaAs NHA and GaAs NHA-DNA, respectively. This result indicated that the thiolated DNA tethered to GaAs NHA surface could result in a dominated passivation effect through the formation of sulfur-GaAs bonds, which coincided with our previously reports (Tang et al. 2013, Yu et al. 2016). We also compared to PL emission for the DNA-modified planar and NHA of GaAs. As shown in Figure 2 (spectra b and e), the peak PL intensity of GaAs NHA-DNA was about 3 times higher than that of GaAs-DNA. This enhanced PL performance can be ascribed to the beneficial features of the nanohorn structures (Mohaddes-Ardabili et al. 2003; Budz et al. 2010, De Luna et al. 2017).

As our previously demonstrated, the DNA duplex-mediated attachment of AuNPs onto GaAs could modulate the PL enhancement of PL intensity of GaAs because of the metal-enhanced fluorescence effect (Yu, Li et al. 2016). In this study, we investigated the influence of AuNRs on the PL intensity. The as-synthesized AuNR had an absorption peak at ~ 650 nm, with an average aspect ratio of 2.5 (Figure S2 and S3 in supplementary materials) (Song et al. 2015). As previously demonstrated, the PL excitation would become most efficient when the laser

excitation wavelength coincides with the maximum plasmon absorption wavelength of AuNRs (Hecker et al. 1999; Barnes, Dereux et al. 2003; Homola 2008; Jin & Gao 2009; Zhang et al. 2010). Thus, it is expected that the AuNRs-over-GaAs systems would display an efficient surface plasmon coupling between GaAs and NPs. The PL spectra in Figure 2 (spectra d and f) show that the AuNRs coating could enhance the PL intensity of both planar and NHA of GaAs, while the enhancement ratio for GaAs NHA was much higher than the one of GaAs, which can be attributed to the 3D nanostructured GaAs have stronger interaction with SP. Therefore, the AuNRs-over-GaAs NHA system had high efficient PL emission, which could be ascribe to their 3D nanostructure and the enhancement from the plasmonic coupling with AuNRs.

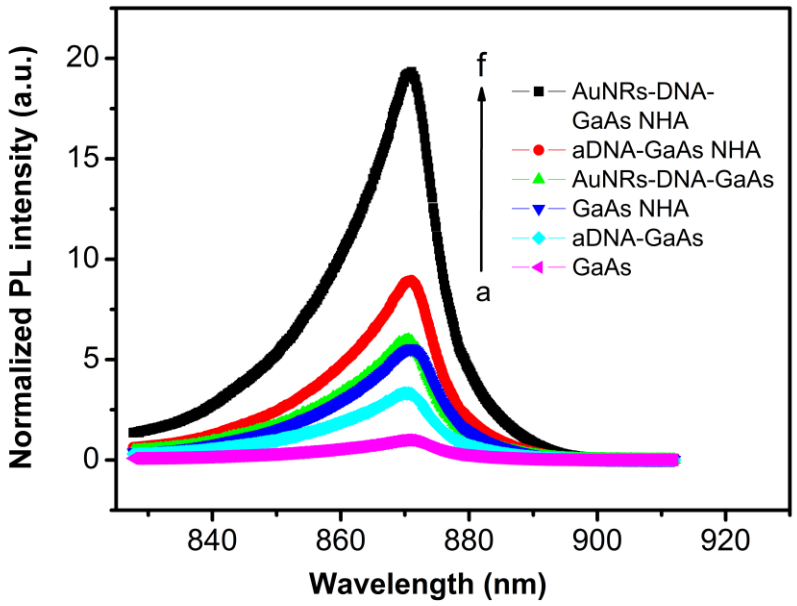


**Figure 2.** PL measurements. (a) GaAs, (b ) aDNA-GaAs, (c) GaAs NHA, (d) AuNRs-DNA-GaAs, (e) aDNA-GaAs NHA and (f) AuNRs-DNA-GaAs NHA. a.u: arbitrary units. The PL peak intensity of untreated GaAs (a) at 875 nm was normalized to 1.

### *3.3 NIR PL detection of DNA using AuNRs-over-GaAs NHA system*

Figure 3A shows the design of AuNRs-over-GaAs NHA-based NIR optical sensor and its operating principle. The surfaces of GaAs NHA were firstly modified with the thiolated pDNA, resulted in the conjugate of pDNA-GaAs NHA. The as-formed substrates were incubated with a tDNA and subsequently immersed into a solution of the eDNA-AuNRs. If the tDNA contains sequences complementary to the pDNA and the eDNA, the AuNRs-over-GaAs NHA hybrid structure would be constructed through the sandwich hybridization of probe-target-enhancer DNAs.

To verify if this system operates correctly, the PL spectra from GaAs were measured by adding complementary and non-complementary tDNAs. Strong enhanced PL signal from GaAs NHA was observed only when the complementary tDNAs were added as seen in Figure 3B (spectrum b), while no obvious signal change was observed even a large excess (micromolar) of non-cognate DNA sequences (Figure 3B, spectrum c), indicating high specificity to DNA sequences. Figure 3C shows the PL signal increased non-linearly with the (logarithmic) concentration of the target, with a detection limit of at least 1 pM (> 3 SD, standard deviation). Noted this sensitivity has been considerably more sensitive than our previous report of GaAs-AuNPs and other systems (Tang, Chun et al. 2013; Guo, Jackman et al. 2015; Zhang et al. 2016b). Also interestingly, while MCH passivation step is critical for the fabrication of planar GaAs-based DNA sensors (if without MCH-backfilling, a 50-fold decrease in sensitivity, 1 pM vs. 250 pM), NHA-based surface with this step could produce comparably PL signal to those treated with MCH (Figure S4 in SI). We attributed this effect to the consistently favorable orientation of DNA probes on nanohorns surface, which avoids possible complications that are often encountered by plain surface and resulted in a high accessibility of DNA recognition onto the DNA probe on the surface (Pei et al. 2010; De Luna, Mahshid et al. 2017).

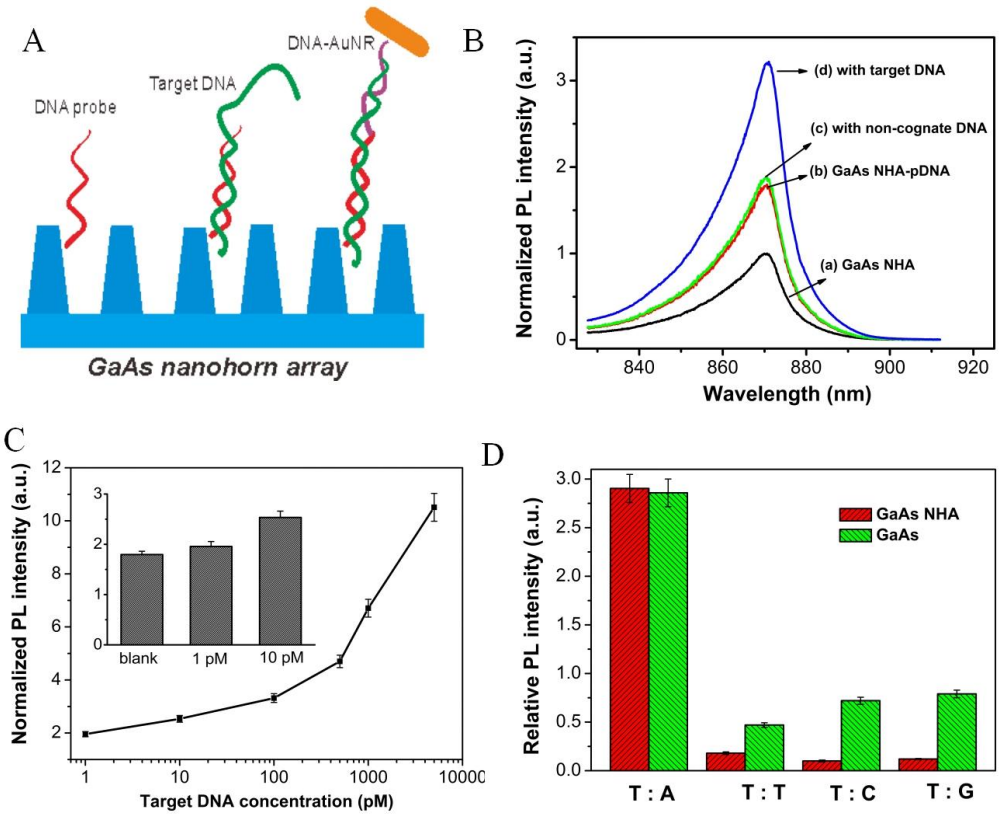


**Figure 3**. GaAs NHA-based DNA NIR optical sensor. (A) The operating principle of DNA sensor. (B) PL measurements of (a) GaAs NHA, (b) GaAs NHA-pDNA, (c) GaAs NHA-pDNA with target DNA (tDNA); (d) GaAs NHA-pDNA with non-cognate DNA. a.u: arbitrary units. . The PL peak intensity of GaAs-NHA at 875 nm was normalized to 1.The PL peak intensity of untreated GaAs (a) at 875 nm was normalized to 1. (C) PL measurements in the presence of target DNA at 0 pM, 1 pM, 10 pM, 100 pM, 1 nM and 5 nM with the AuNRs-over-GaAs NHA sandwich mode. (D) Comparison for the single-base mismatch discrimination ability of a GaAs NHA-based sensor and a planar GaAs-based sensor for different mutant types. The single-base pair mismatched DNA:5'-GC TAG AGA TXT TCC ACA CTG ACT-3' (X: A, C or G). All target concentrations are 1 nM. Relative PL intensity (ΔPL) of GaAs at ~875 nm compared to the pDNA-GaAs NHA. The error bars correspond to the standard deviation of PL measurements across 8~10 repetitive experiments.

Single nucleotide polymorphisms represent promising genetic biomarkers to disease because they are stably inherited sequence variations in the human genome (Ogasawara & Fujimoto 2006; Subramanian et al. 2011). Importantly, we found that AuNRs-over-GaAs NHA system exhibited remarkable selectivity for single-base mismatches (Figure 3D). The discrimination factors

between a fully complementary (A:T) and three internal single-base mismatched targets were 20:1, respectively. Parallel studies with the AuNRs-over-planar GaAs sensors showed much weaker selectivity, with SNP discrimination factors of 5:1, respectively. As for the enhanced ability to discriminate SNP for GaAs NHA substrates, we supposed that the nanohorns GaAs array would provide more favorable spatial positioning range and accessibility of the probes on a surface over plain surface. Therefore, a three-dimensional (3D) nanostructured GaAs surface would be ideally suited for this biosensing system (Soleymani, et al. 2009).

### *3.4 NIR PL detection of thrombin using AuNRs-over-GaAs NHA system*

Aptamer, as an emerging class of DNA molecules, has been selected against the target of interest for specific and effective binding, allowing for the use of multiple aptamers to develop sandwich-based target capture and reporting (Zhou & Rossi 2016). In the present work, a novel aptamer-based protein detection strategy using AuNRs-over-GaAs NHA sensing platform was proposed, as schematically shown in Figure 4A. Thrombin-binding aptamers (TBA) were chosen as a model system to provide the "proof-of-principle" verification of the concept (Chen et al. 2016; Fan et al. 2016; Trapaidze et al. 2016; Wang et al. 2016; Zhang, Ren et al. 2016b). In a typical experiment, two different thrombin-binding aptamers (TBA15 and TBA29), selectively binding to specific and different epitopes of human α-thrombin, were first immobilized onto the GaAs NHA and AuNRs, respectively. Upon adding thrombin, the specific recognition between thrombin and TBA was expected to induce the formation of the AuNRs-over-GaAs NHA architecture and thus result in an enhanced PL emission of GaAs, allowing for the sensitive and specific detection of thrombin.

To evaluate the performance of such a sandwich assay system, we investigated the PL response to different concentrations of the target thrombin. As shown in Figure 4B and 4C, the

PL peak intensity gradually increased as the increase of the thrombin concentration correspondingly. According to the definition that the detection limit is the lowest analytes concentration required to produce a signal greater than 3 times the standard deviation of the noise level (3α), the limit of detection (LOD) for this system was estimated to be 10 pM (~36 pg/mL, given the molecular weight of thrombin is ~36,000). This LOD is comparable to or rivals current bioanalytical methods such as ELISA (enzyme-linked immunosorbent assay) and PLA (proximity ligation assay), which typically detects analytes with concentration ranging from pM to nM. With comparison to those aptamer-based sensing systems which integrated with colorimetric, luminescent, fluorescent, and electrochemical techniques (Table S1 in SI), our system represents a 1 to 1000-fold improvement in term of sensitivity, together with a wide linear dynamic range(Shiang et al. 2010; Yuan et al. 2014; Fan, Guo et al. 2016; Trapaidze, Herault et al. 2016; Zhang et al. 2016a; Zhang, Ren et al. 2016b).

To evaluate the specificity, control and recovery experiments were performed using other proteins including immunoglobulins G (IgG, 1 μM), bovine serum albumin (BSA, 1 μM) and biotin (1 μM) in PBS solution, and thrombin in the complex matrices (50% goat serum or buffer solution containing other multiple proteins). As shown in Figure 4D and Figure S5 in supplementary materials, these control groups exhibited minimal signals which are close to the non-target background. We also spiked different concentration of thrombin in serum, and then determined the concentrations of the proteins in the spiked samples (Figure 4E. The recoveries were 90% ~ 95%, indicating that our assay possesses a great selectivity and anti-interference capability even in complex matrix and may therefore find practical utility in clinical settings. Although thrombin was used as a model protein here to demonstrate the feasibility of this design, a wide range of aptamer-based ligands rather than proteins, could be detected using the approach.

Moreover, by optimizing the experimental conditions and integrating with microfluidics systems, it is anticipated that a significantly enhanced sensitivity, multiplexed and high-throughput detection could be achieved, which may provide versatile platform for the detection of a broad range of biomolecules.

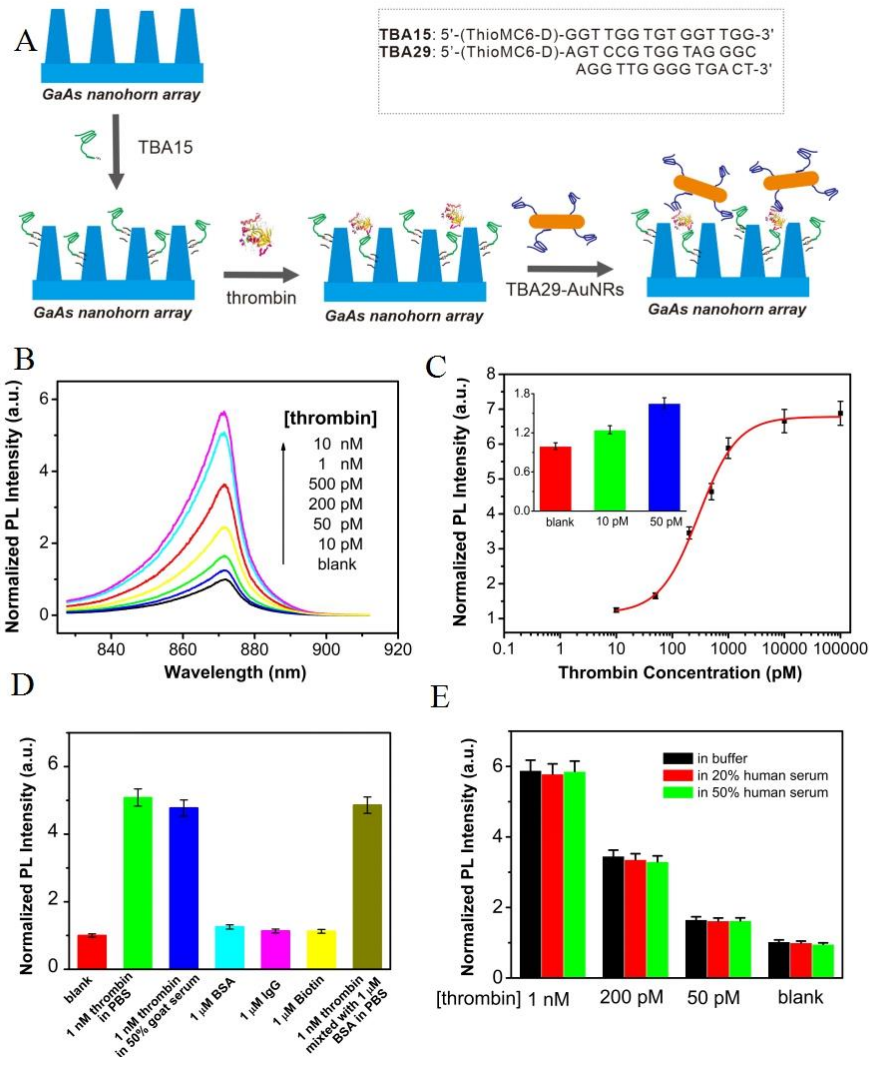


**Figure 4** (A) Schematic representation of the aptamer-based NIR optical sensor using AuNRs-over-GaAs system. (B) Typical PL response and intensity change of GaAs NHA to different concentration of thrombin from 10 pM to 10 nM. (D, E) PL intensity change at 875 nm of GaAs NHA in the presence of 1 nM target thrombin and 1 μM other species of proteins and different concentration of thrombin in the PBS solution or diluted goat serum samples, respectively. The error bars correspond to the standard deviation of PL measurements across five repetitive experiments.

## CONCLUSION

To sum up, we have demonstrated that the AuNRs-over-GaAs NHA system using DNA scaffold as a bridge can be employed as NIR optical biosensing platform for the specific and sensitive detection of the biomarkers, such as DNA and thrombin. Compared to other conventional optical sensing systems, this AuNRs-over-GaAs NHA platform possesses several unique features, resulting in the improved sensing performance. First, the AuNRs-over-GaAs NHA system provides reproducible and significantly improved PL signals, which originate from the uniform well-ordered nanostructured GaAs and AuNRs-enhanced PL effect. Second, the GaAs NHA with 3D well-ordered nanostructure has more advantageous on the surface sensing. The NHA functionalized with molecular probes can be more readily and reliably recognized with the targets compared to the planar surface, because the nanohorns-like nanostructure should provide a significantly enhanced spatial positioning range and increased accessibility of the target molecules to the surface probes (De Luna, Mahshid et al. 2017). Third, the system can be directly employed in the detection of targets for biological fluids (e.g., serum), because of the NIR PL sensing model and high protein resistance ability. Fourth, as its basis on the solid substrate, this sensing platform is fully compatible with microarray chip system, providing opportunities to develop multiplexing and high through-put analysis. In addition, the sensor design can be easily extended to the immunosensing scheme such as the enzyme-linked immunosorbent assay (ELISA), which may provide a highly versatile platform for the detection of other molecules. Given these advantages, we believe this AuNRs-over-GaAs NHA sensing platform are greatly promising in the NIR optical biosensor design and significantly further the field of chip-based biomolecular detection.

## ASSOCIATED CONTENT

### Supporting Information.

Experimental details for the characterizations of the as-prepared AuNRs, GaAs NHA and PL spectra of NHA.

### Notes

The authors declare no competing financial interest. Acknowledgement

## ACKNOWLEDGMENT

This work was financially supported by National Natural Science Foundation of China (No. 61405176), Natural Sciences Fund of Zhejiang Province (No. LY14B050004) the Scientific Research Start-up Fund of Zhejiang Agriculture and Forestry University (No. 2015FR012), the Scientific and Technology Project for Analysis and Test of Zhejiang Provincial Department of Technology (No. 2015C37071) and the Fundamental Research Funds for the Central Universities (No. 2016QNA5001). Y.M.Z. and T.J. contributed equally to this work.



## REFERENCES

Barnes, W. L., A. Dereux & T. W. Ebbesen 2003, Nature, 424, 824.

Boghossian, A. A., J. Zhang, P. W. Barone, N. F. Reuel, J. H. Kim, D. A. Heller, J. H. Ahn, A. J. Hilmer, A. Rwei and J. R. Arkalgud 2011, ChemSusChem, 4, 848.

Budz, H. A., M. M. Ali, Y. Li & R. R. LaPierre 2010, J Appl Phys, 107, 104702.

Chen, L. Y., Y. G. Bao, J. Denstedt & J. Zhang 2016, Biosens Bioelectron, 77, 83.

Chun, I. S., K. Bassett, A. Challa & X. Li 2010, Appl Phys Lett, 96, 251106.

Connolly, A. R. & M. Trau 2010, Angewandte Chemie International Edition, 122, 2780.

Dai, Z., Y. Li, G. Duan, L. Jia & W. Cai 2012, Acs Nano, 6, 6706.

De Luna, P., S. S. Mahshid, J. Das, B. Luan, E. H. Sargent, S. O. Kelley & R. Zhou 2017, Nano Letters, 17, 1289.

Fan, D. W., C. J. Guo, H. M. Ma, D. Zhao, Y. N. Li, D. Wu & Q. Wei 2016, Biosens Bioelectron, 75, 116.

Fortuna, S. A., J. Wen, I. S. Chun & X. Li 2008, Nano Letters, 8, 4421.

Gao, X., Y. Cui, R. M. Levenson, L. W. K. Chung & S. Nie 2004, Nat Biotech, 22, 969.

Gopinath, S. C. B., T. H. Tang, M. Citartan, Y. Chen & T. Lakshmipriya 2014, Biosens Bioelectron, 57, 292.

Guo, L. H., J. A. Jackman, H. H. Yang, P. Chen, N. J. Cho & D. H. Kim 2015, Nano Today, 10, 213.

Hecker, N., R. Höpfel, N. Sawaki, T. Maier & G. Strasser 1999, Appl Phys Lett, 75, 1577.

Hilderbrand, S. A. & R. Weissleder 2010, Current Opinion in Chemical Biology, 14, 71.

Homola, J. 2008, Chemical Reviews, 108, 462.

Hong, G., A. L. Antaris & H. Dai 2017, Nature Biomedical Engineering, 1, 0010.

Howes, P. D., S. Rana & M. M. Stevens 2014, Chemical Society Reviews, 43, 3835.

Jin, Y. & X. Gao 2009, Nature Nanotechnology, 4, 571.

Lim, W. Q. & Z. Q. Gao 2016, Nano Today, 11, 168.

Liu, J., Z. Cao & Y. Lu 2009, Chemical Reviews, 109, 1948.

Liu, N., Y. Hu & J.-J. He 2014, Piers Proceedings, 959.

Malic, L., M. G. Sandros & M. Tabrizian 2011, Anal Chem, 83, 5222.

Mohaddes-Ardabili, L., L. J. Martínez-Miranda, J. Silverman, A. Christou, L. G. Salamanca-Riba, M. Al-Sheikhly, W. E. Bentley and F. Ohuchi 2003, Appl Phys Lett, 83, 192.

Ogasawara, S. & K. Fujimoto 2006, Angewandte Chemie International Edition, 45, 4512.

Okamoto, K., I. Niki, A. Shvartser, Y. Narukawa, T. Mukai & A. Scherer 2004, Nat Mater, 3, 601.

Pei, H., N. Lu, Y. Wen, S. Song, Y. Liu, H. Yan & C. Fan 2010, Advanced Materials, 22, 4754.

Resch-Genger, U., M. Grabolle, S. Cavaliere-Jaricot, R. Nitschke & T. Nann 2008, Nat Meth, 5, 763.

Rosini, M. & R. Magri 2010, ACS Nano, 4, 6021.

Shahbazyan, T. V. 2012, Nano Letters, 13, 194.

Shiang, Y.-C., C.-C. Huang, T.-H. Wang, C.-W. Chien & H.-T. Chang 2010, Adv Funct Mater, 20, 3175.

Smith, S. J., C. R. Nemr & S. O. Kelley 2017, J Am Chem Soc, 139, 1020.

Soleymani, L., Z. Fang, X. Sun, H. Yang, B. J. Taft, E. H. Sargent &S. O. Kelley, 2009, Angewandte Chemie International Edition 48, 8457

Song, T., L. Tang, L. H. Tan, X. Wang, N. S. R. Satyavolu, H. Xing, Z. Wang, J. Li, H. Liang and Y. Lu 2015, Angewandte Chemie International Edition, 54, 8114.

Song, Y. J., Y. Y. Huang, X. W. Liu, X. J. Zhang, M. Ferrari & L. D. Qin 2014, Trends in Biotechnology, 32, 132.

Subramanian, H. K. K., B. Chakraborty, R. Sha & N. C. Seeman 2011, Nano Letters, 11, 910.

Tang, L., I. S. Chun, Z. Wang, J. Li, X. Li & Y. Lu 2013, Anal Chem, 85, 9522.

Trapaidze, A., J. P. Herault, J. M. Herbert, A. Bancaud & A. M. Gue 2016, Biosens Bioelectron, 78, 58.

Wang, Y. G., Y. Zhang, T. Yan, D. W. Fan, B. Du, H. M. Ma & Q. Wei 2016, Biosens Bioelectron, 80, 640.

Yu, F., Y. Li & L. Tang 2016, Optik - International Journal for Light and Electron Optics, 127, 11492.

Yuan, F., H. Q. Chen, J. Xu, Y. Y. Zhang, Y. Wu & L. Wang 2014, Chem-Eur J, 20, 2888.

Zhang, H., Y. J. Li, I. A. Ivanov, Y. Q. Qu, Y. Huang & X. F. Duan 2010, Angewandte Chemie-International Edition, 49, 2865.

Zhang, H., C. X. Wang, G. Wang, K. Wang & K. Jiang 2016a, Biosens Bioelectron, 78, 344.

Zhang, Y., W. Ren, H. Q. Luo & N. B. Li 2016b, Biosens Bioelectron, 80, 463.

Zhou, J. & J. Rossi 2017, Nat Rev Drug Discov, 16, 181.

Zhou, X., Q. Wei, L. Wang, B. Joshi, Q. Wei & K. Sun 2009, Appl Phys A, 96, 637.

Highlights

- The large-area and well-defined nanohorn-like GaAs array was developed using colloidal nanoparticles-templated etching technique.
- The DNA-bridged gold nanorods-over-GaAs nanohorn array system provided a reproducible and improved PL signals and had high bio-recognition activity.
- 3. The ultrasensitive near-infrared optical detection of DNA and thrombin was realized using the above biosensing platform.